BMC Plant Biology

RESEARCH

Open Access

Genome-wide identification and analysis of phosphate utilization related genes *(PURs)* reveal their roles involved in low phosphate responses in *Brassica napus* L.

Yibing Shen[1,2], Jiaqi Chen[1,2], Haijiang Liu[1,2], Wenyu Zhu[1,2], Zhuo Chen[1,2], Li Zhang[1,2], Runjie Du[1,2], Zexuan Wu[1,2], Shiying Liu[1,2], Sining Zhou[1,2], FuminYuan[1,2], Huiyan Zhao[1,2], Nengwen Yin[1,2], Jiana Li[1,2], Cunmin Qu[1,2*] and Hai Du[1,2*]

Abstract

Background Phosphorus (P) is an essential macronutrient for *Brassica napus* L. growth and development, and is mainly acquired from the soil as phosphate (Pi). However, there is no research on the system analysis of Pi utilization related genes (*PURs*) in *B. napus* yet.

Results In this study, 285 *PURs* were identified in *B. napus* genome, including 4 transcription factor (TF) gene families (83 genes) and 17 structural gene families (202 genes). Subcellular localization analysis showed that the proteins encoded by *B. napus PURs* were mainly located in the nucleus (~46.0%) and cell membrane (~36.5%). Chromosome localization analysis suggested that *B. napus PURs* were distributed on An (131) and Cn (149) subgenomes without bias. Analysis of 35 representative species confirmed that *PURs* were widely present in plants ranging from Chlorophyta to angiosperms with a rapid expansion trend. Collinearity analysis revealed that allopolyploidization and small-scale duplication events resulted in the large expansion of *B. napus PURs*. For each gene pair of *B. napus PURs*, the sequence identity of promoter was significantly lower than that of CDS, proving the significant difference in promoter region that might be related to the divergence of *PURs* expression and function. Transcription factor (TF) binding site prediction, cis-element analysis, and microRNA prediction suggested that the expressions of *B. napus PURs* are regulated by multiple factors including 32 TF gene families (362), 108 types of CRE (29,770) and 25 types of miRNAs (66). Spatiotemporal expression analysis demonstrated that *B. napus PURs* were widely expressed during the whole developmental stages, and most synteny-gene pairs (76.42%) shared conserved expression patterns. RNA-seq analyses revealed that most *B. napus PURs* were induced by low Pi stress, and the hub genes were generally the Pi transporter (PHT) family members. qRT-PCR analysis proved that the expression levels of four *B. napus PURs* were positively correlated with the root system architecture of three *B. napus* varieties under low Pi supply at the seedling stage.

*Correspondence:
Cunmin Qu
drqucunmin@swu.edu.cn
Hai Du
haidu81@126.com
Full list of author information is available at the end of the article

Conclusion The 285 *PURs* were identified from *B. napus* with strong LP inducible expression profile. Our findings regarding the evolution, transcriptional regulation, and expression of *B. napus PURs* provide valuable information for further functional research.

Keywords *Brassica napus*, Phosphate, Gene network, Evolution, Expression

Background

Phosphorus (P) is an essential macronutrient for plant growth and development which is acquired by plants as inorganic phosphate (Pi), and fulfills diverse functions in plants including energy metabolism, photosynthesis, signal transduction, energy, information storage or transfer, etc. [1, 2]. Due to the high rate of chemical fixation and slow diffusion in the soil, Pi deficiency in cultivated soil often restricts crop production [3]. To support population development and increase yield, P fertilizer is excessively used in crop production worldwide. However, this generally causes many environmental problems [4]. Thus, for sustainable agricultural production, improving crop Pi utilization efficiency (PUE) is an imperative issue.

During the course of evolution, plants have evolved a complex mechanism and pathway to control Pi utilization, mainly including the acquisition, redistribution/translocation, mobilization, and homeostasis processes, controlled by a set of regulatory genes and structural genes in a coordinated manner [3]. In plants, Pi acquisition and transport processes are primarily controlled by the five members of the Pi transporter family (PHT1-5), where the PHT1 family plays a key role in Pi uptake from the soil, while PHT2-5 families are mainly involved in the subcellular Pi transport [5–7]. Subsequently, the Pi is translocated into vascular bundles through apoplast and simplistic nutrient transport pathways, then is uploaded into the xylem to deliver to the shoot by PHO1 [8]. Pi can be redistributed between different tissues or organs according to the demands [9]. During these processes, excess Pi will be stored in the vacuoles, maintaining the cellular Pi homeostasis [10]. Besides the structural genes, many transcription factor genes (*TFs*) are involved in the Pi utilization process, such as members of the MYB, WRKY gene families, etc. [11, 12]. Meanwhile, SPX proteins [13, 14] and microRNAs (e.g., miR156, miR399) [15, 16] also play important regulating roles in the Pi utilization process by guiding the cleavage of transcripts from target genes. Furthermore, to maintain Pi homeostasis, Pi transporters might undergo regulation at the post-translational level through either the protein's abundance or its subcellular localization. For instance, members of the PHF1 family facilitate the movement of Pi transporters to the plasma membrane [17]. The genes from the PHO2 family are responsible for encoding ubiquitin-conjugating (UBC) E2 enzymes, which suppress the quantities of Pi transporter proteins (including PHT1, PHO1, and PHF1) [18–22]. Together, PUE is determined by Pi utilization related genes (*PURs*) in plants, and vast genes involved in PUE have functionally characterized in plant species, especially Arabidopsis [7, 8, 11, 13, 14]. Undoubtedly, exploring and understanding the whole gene network of PUE in crop genomes is fundamental for enhancing *PURs* through molecular strategies.

Brassica napus L. ($A_nA_nC_nC_n$, 2n = 38) is one of the worldwide polyploid crops derived from *Brassica rapa* (A_rA_r, 2n = 20) and *Brassica oleracea* (C_oC_o, 2n = 18) hybridization [23, 24], its oil-rich seeds are used for both nutritional and industrial applications [25]. Its growth and development and yield are susceptible to Pi condition. However, the gene, gene network, and molecular regulatory mechanism of the Pi utilization process in *B. napus* is largely unknown yet. Therefore, identification of *PURs* at a genome-wide scale and investigation of their functions in Pi utilization in *B. napus* will have potential academic and application values.

In this study, we first identified and characterized *PURs* in *B. napus*, *B. rapa*, and *B. oleracea* genomes to explore the evolution mechanism of the gene network. And we investigated the potential regulators of *B. napus PURs*, including TFs and miRNAs. Consequently, we analyzed the spatiotemporal expression profiles of *PURs* in 90 samples across different developmental stages of *B. napus*. Meanwhile, the low P (LP) stress expression profile and co-expression network of *B. napus PURs* were investigated. Finally, the expression pattern of four candidate *PURs* under LP condition in three *B. napus* varieties with different root system architecture (RSA) were analyzed. The present work provides a comprehensive overview and assessment of the distribution, evolution, and expression patterns of *PURs* in *B. napus*.

Materials and methods

Genome-wide identification of *PURs* in *B. napus* genome

The protein sequences of known *Arabidopsis* and *Oryza sativa PURs* were obtained from TAIR (https://www.arabidopsis.org/) and Phytozome v12 (https://phytozome-next.jgi.doe.gov/). To identify *PURs* in *B. napus* genome, a BLASTP search was conducted against the proteome database of *B. napus* Zhongshuang 11 (ZS11) in BnIR (https://yanglab.hzau.edu.cn/BnIR) using *Arabidopsis*

and rice *PURs* as queries, respectively. Only hits with E-values < 1.0 were considered as the candidate *B. napus PURs*. To ensure the reliability of the results, candidate sequences were further validated using SMART (http://smart.emblheidelberg.de/) and PROSITE (https://prosite.expasy.org/) to confirm the presence of characteristic domains of each gene family. The same procedure was used to identify the candidates in *B. rapa* and *B. oleracea* genomes in Phytozome (https://phytozome-next.jgi.doe.gov/). The DNA, CDS, promoter, and protein sequences of candidates were acquired from the corresponding genome databases as well. Subcellular localization was predicted by Cell-PLoc2.0 (http://www.csbio.sjtu.edu.cn/bioinf/Cell-PLoc-2/), WoLF PSORT (https://wolfpsort.hgc.jp/) and Protein Prowler version 1.2 (http://bioinf.scmb.uq.edu.au:8080/pprowler_webapp_1-2/index.jsp) with default settings, respectively.

The same procedure and criteria were followed to identify the homologs from another 33 sequenced plant genomes in Phytozome (http://www.Phytozome.net), including algae (*Porphyra umbilicalis, Volvox carteri, Chlamydomonas reinhardtii, Chara braunii* and *Klebsormidium nitens*), moss (*Marchantia polymorpha, Sphagnum fallax,* and *Physcomitrella paten*), tracheophytes (*Selaginella moellendorffii* and *Diphasiastrum complanatum*), gymnosperms (*Ginkgo biloba* and *Pinus taeda*), basal magnoliophyta (*Amborella trichopoda* and *Nymphaea colorata*), monocots (*Zea mays* and *Oryza sativa*), and eudicots (*Aquilegia coerulea, Eschscholzia californica, Solanum lycopersicum, Solanum tuberosum, Daucus carota, Mimulus guttatus, Eucalyptus grandis, Vitis vinifera, Malus domestica, Prunus persica, Citrus sinensis, Citrus clementina, Gossypium raimondii, Brassica rapa, Brassica oleracea, Glycine max,* and *Medicago truncatula*).

Chromosomal localization and collinearity analysis of *PURs* in *B. napus*

The GENOSCOPE database (http://www.genoscope.cns.fr/brassicanapus/) was applied to collect the chromosome and gene location information of candidate *B. napus PURs* as well. The collinearity relationship of *PURs* in *B. napus*, *B. oleracea*, and *B. rapa* was analyzed by CoGe online software (https://genomevolution.org/coge/). The duplication events were determined based on the analysis of cross-genome collinearity analysis among candidates (orthologous gene pairs in orthologous blocks), which employed the specific methods in our previous research [26]. Homeologous exchanges (HE) and segmental exchanges (SE) referred to transfer of genetic information between homeologous sequences of different subgenomes and segmental exchanges transfer of genetic information between different chromosomal sequences, respectively. Segmental duplications (SD) were determined as duplicated copies of chromosomal sequences. Tandem duplicated genes (TD) were defined as closely related genes within a single cluster in the phylogenetic tree that was physically localized adjacent to each other on a given chromosome with no more than one intervening gene. The nucleotide substitution rate (Ka/Ks) of *B. napus PURs* was calculated by KaKs_calculator2.0, using the Locally Weighted Learning (LWL) method [27]. To ensure the accuracy of the results, the values with p-value > 0.05 were excluded.

Promoter and miRNA regulation, and protein interaction networks of *PURs* in *B. napus*

PlantCARE (http://bioinformatics.psb.ugent.be/webtools/plantcare/html/) and PlantTFDB online software (http://planttfdb.cbi.pku.edu.cn/prediction.php) are used to predict the potential *cis*-acting regulatory elements and putative TF-binding sites (a threshold p-value < 1e-7) in −1,500 bp upstream promoter regions of *B. napus PURs* respectively. And psRNATarget (http://plantgrn.noble.org/psRNATarget/analysis?function=2) was employed to predict potential regulatory miRNAs in the CDS sequences of *B. napus PURs* with default parameters (expectation ≤ 5). The results were visualized by Cytoscape software [28].

Development and low Pi stress expression profiles of *PURs* in *B. napus*

The data used for spatiotemporal expression profile analysis of *PURs* was obtained from the website BnIR (https://yanglab.hzau.edu.cn/BnIR), covering 90 samples from different tissues/organs (including cotyledons, roots, stem bark, leaves, shoots, flowers, longhorn fruit, longhorn fruit wall and seeds) at three developmental stages of *B. napus* cultivar 'Zhongshuang 11'(ZS11). The low Pi stress expression profile of *PURs* in *B. napus* was analyzed based on the low Pi stress treatment transcriptome data from BnGADB (http://www.BnaGADB.cn), which contained data for roots and leaves after 1, 3, 5, 7, and 12 days of low Pi treatment. The genes having no or weak expression value (FPKM < 1) were considered a pseudogene or expressed under special conditions, thereby were excluded for technical reasons. All of the RNA-Seq data (FPKM ≥ 1) of *B. napus PURs* were log2-transformed, and then the heatmap was drawn by the "pheatmap" package in R language.

Co-expression analysis of *PURs* in *B. napus*

The "psych" package in R language was applied to calculate the correlation between the expression patterns of *PURs* with Pearson Correlation Coefficient ≥ 0.6 and p-value ≤ 0.01, based on the above *B. napus*

spatiotemporal and low Pi stress expression datasets. The results were visualized by Cytoscape software [27]. The MCODE plugin in Cytoscape was employed to calculate the core gene network with default parameters. The cytoHubba plugin was used to identify hub genes within each gene network with default parameters. The top ten genes were subsequently selected based on the high degree values.

Plant materials and growth condition

Three *B. napus* varieties (226, 252, and 470) with different RSA under low Pi supplement were selected to assess the expression patterns of *PURs* [29]. The seeds were obtained from the College of Agriculture and Biotechnology, Southwest University. Firstly, the seeds were disinfected with 10% sodium hypochlorite solution and 75% alcohol for five minutes, respectively, and rinsed twice with pure water. Then, the rinsed seeds were germinated for two days on Petri dishes containing Hoagland solid media (Coolaber, Beijing, China). Next, healthy seedlings were transferred into Petri dishes containing phosphorus-deficient Hoagland's solid medium (Coolaber, Beijing, China). The seedlings were grown in the plant tissue culture laboratory at 22 °C with a 16/8 h (day/night) photoperiod. Roots were collected on 4, 7, and 12 days after P deficient treatments and immediately frozen in liquid nitrogen, respectively. Three biological replicates were performed for each time point, and five plants were used in each replicate. All samples were stored at − 80 °C for RNA extraction.

qRT-PCR analysis of *PURs* under LP condition in different *B. napus* varieties

The qRT-PCR method was further applied to analyze the expression levels of four putative low Pi stress responsive *B. napus PURs* in the above three varieties under LP condition, using *BnActin2* as control. The primers of candidate *B. napus PURs* and *BnActin2* used in this analysis were listed in Table S1. The RNA simple total RNA Extraction Kit (TIANGEN, Beijing, China) was used to extract the total RNA in each sample. Then, the quality and concentration of the total RNA were examined using 1% gel electrophoresis and a Thermo Fisher ScientificTM spectrophotometer (Thermo, Beijing, China), respectively. Subsequently, about 1.0 μg of the total RNA was applied to synthesize first-strand cDNA in a 20 μL reaction system, according to the manufacturer's instructions of HiScript ® III RT SuperMix for qPCR (+ gDNA wiper) HiScript ® III RT kit (Vazyme, Nanjing, China). The Taq Pro Universal SYBR qPCR Master Mix Kit (Vazyme, Nanjing, China) was used to perform the Real-time PCR analysis in a CFX Connect ™ Real-Time System (Bio-Rad, USA). Each treatment contained three biological replicates, whereas each replicate had three technical replicates. The $2(^{-\Delta\Delta Ct})$ method was used to calculate the relative gene expression levels of candidates. The one-way ANOVA analyses of variance (*: $0.01 < p < 0.05$; **: $p < 0.01$) (Excel 2016) were used to assess the difference in the expression level of each gene.

Results

PURs were widely distributed in *B. napus* genome and experienced a complex evolution process across land plants

We identified 285 *PURs* in the *B. napus* ZS11 ecotype genome, belonging to five TF gene families (*bHLH, PHR, WRKY, SPX, NIGT1*; 83 genes) and 16 structural gene families (202 genes) (Table S2). Subcellular localization analysis (Table S2) showed that PURs are mainly localized in the nucleus or the cell membrane, while a few proteins were localized in chloroplasts, vesicles, mitochondria, cytoplasm, and endoplasmic reticulum (Table S2). The proteins belonging to the same gene family are usually localized in the same subcellular structures, indicating their functional conservation and relevance, and also reflecting the division of labor and feedback mechanism of PURs in cells, which may have a close correlation with PUE in *B. napus*. Chromosome localization analysis showed that 280 *PURs* were scattered on all 19 *B. napus* chromosomes, excluding five genes with uncertain chromosome locations (Table S2, Fig. 1). The numbers of *PURs* on the C_n-subgenome (149 genes) and A_n-subgenome (131 genes) showed a biased trend, with more genes on C_n-subgenome. Moreover, the number of *PURs* on each chromosome was uneven (Figure S1), the most genes (31 genes) were located on A09, while the least were on A05 (five genes). *PURs* are generally distributed at the ends of each chromosome, with some of them forming gene clusters.

To evaluate the distribution and expansion trends of *PURs* in plants, we broadened our dataset to cover more representative plant lineages (35 species), ranging from aquatic algae to angiosperms (Fig. 1B, Table S3). A total of 3,588 Pi utilization-related homologs from the 23 gene families were obtained (Table S3). We found that *PURs* were present earlier in Chlorophyta, and showed a rapid gene expansion trend from aquatic alga to angiosperms. For example, only 11 homologs were encoded in single-celled chlorophytes, *C. reinhardtii*, while 68 homologs were present in moss (*P. patens*) and up to 285 homologs in *B. napus*. Overall, the evolution and expansion of *PURs* in plants may be divided into three major stages. The first stage representing the origin of the main structural genes (10 of the 17 types of homologs) occurred at least in Chlorophyta. At this stage, the primary structural gene family of Pi acquisition and transport (PHT)

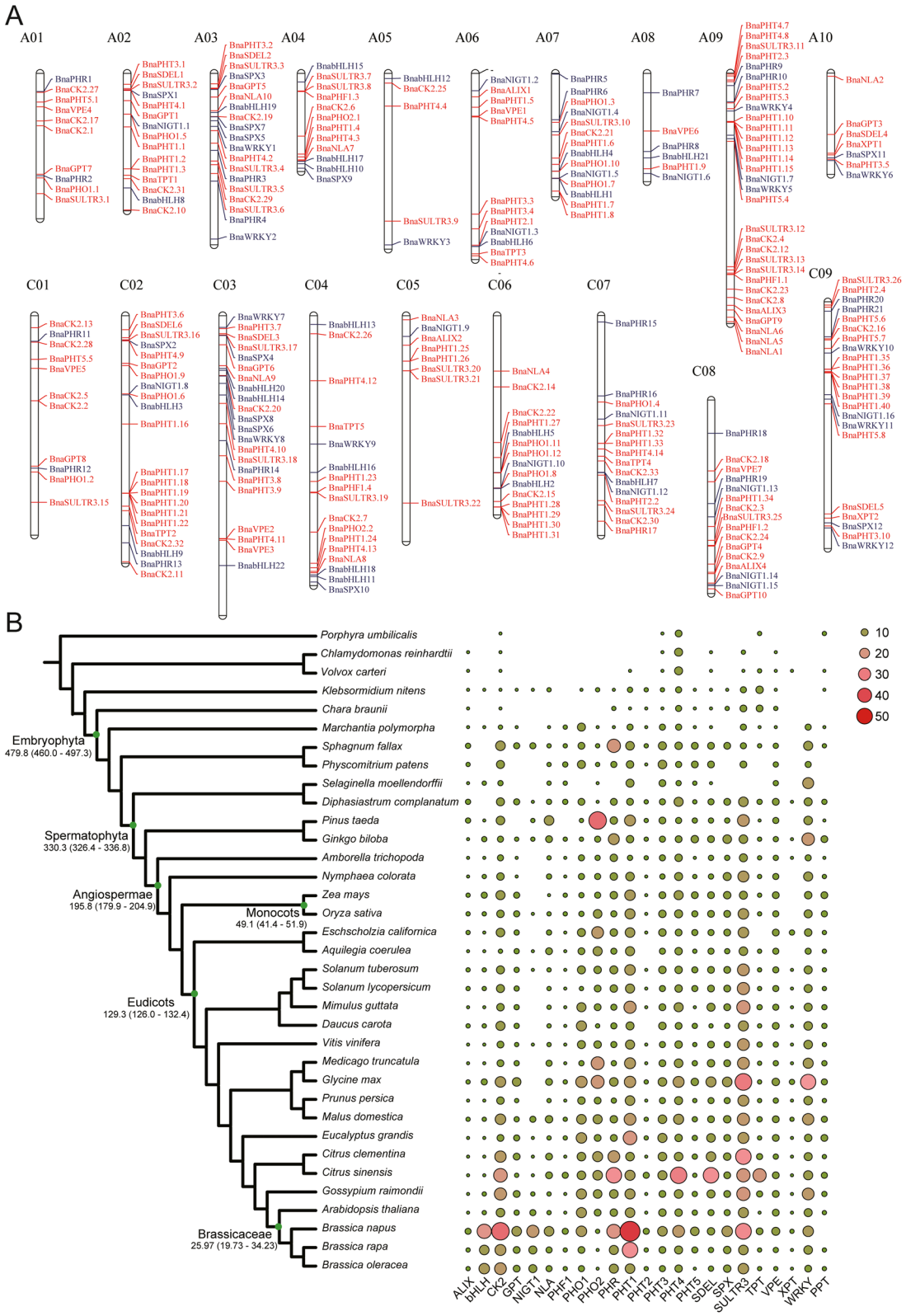

Fig. 1 The distribution of *PURs* in land plants. **A** Chromosome mapping of the *PURs* in *B. napus*. The red and black lines represent *TFs* and the structural genes, respectively. **B** The distribution of *PURs* in 35 typical plant species. Homologous genes are marked at the bottom. The numbers at the branches of the evolutionary tree represent differentiation time in million years ago (MYA), with the time range in parentheses

had already originated. The second stage represents the establishment of the main regulatory genes in Pi utilization pathway at the very beginning of the transition from aquatic to terrestrial plants. At this stage, the majority of structural genes related to Pi utilization, especially CK2, PHO1, PHT1-5, SDEL and SULTR3 gene families, and all of the 6 TF families, had emerged in basal land plants. Thus far, the Pi utilization system had become more precise, consistent with the morphology and structural complexity of land plants evolved from aquatic to terrestrial forms. There was an extensive gene expansion in *Sphagnum fallax* with the number of some genes (e.g., CK2 and PHR) were significantly increased, indicating the wide roles of CK2 and PHR genes in *Sphagnum fallax* utilizing Pi. In gymnosperms, the numbers of *PURs* reached 110 and 127, which were higher than both tracheophytes and basal magnoliophyte. This result implied that there existed significant *PURs*'replication and loss during the process. The third stage represents perfection of Pi utilization pathway early in basal angiosperm, *A. trichopoda*. The types, instead of the number, of structural genes in *PURs* were highly conserved in angiosperms during evolution; by contrast, the types and number of the regulatory genes were still increasing, and the homologs of many regulatory genes (e.g.,PHR and WRKY) emerged first, leading to a more complex gene network in angiosperms, suggesting that regulatory genes are the factors underlying low Pi tolerance in different plants/crops. The wide distribution and expansion of *PURs* along with plant evolution also indicate the complex evolutionary process and gene regulatory network in *B. napus*.

Collinearity relationship and evolution mechanisms of *PURs* in *B. napus*

Collinearity analysis revealed that 257 of the 285 (~90.18%) *B. napus PURs* had a collinearity relationship in at least one of *B. oleracea*, *B. rapa,* and *B. napus* genome. The rest (28, ~9.82%) cannot detect syntenic relationships (Table S4, Fig. 2A). Among the 257 *B. napus PURs*, ~30.35% (78 genes) were inherited from *B. rapa* (69; ~26.85%) and *B. oleracea* (9; ~3.50%) via the allopolyploid event between the two ancestors (Fig. 2B and 1C). Small-scale duplication events, including segmental duplication (SD; 101 genes; ~39.30%), homologous exchange (HE; 58 genes; ~22.57%), and segmental exchange (SE; 20 genes; ~7.78%), were found to play an

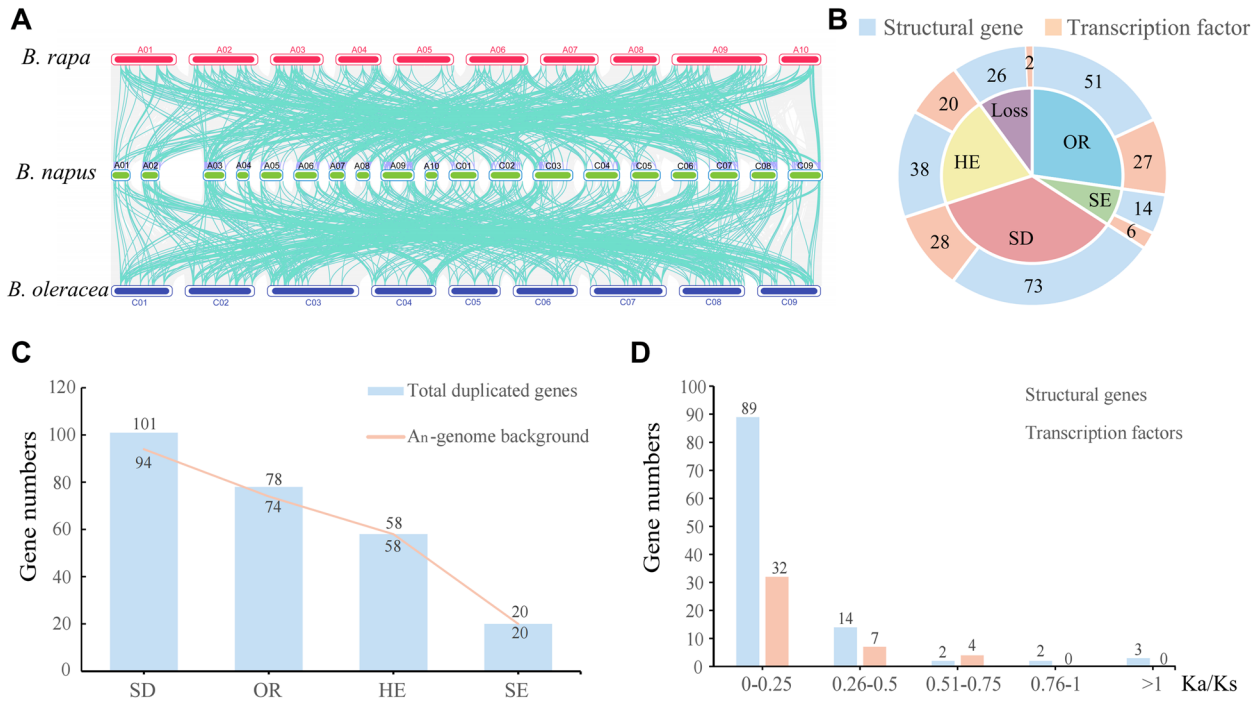

Fig. 2 Syntenic relationship and evolution mechanism of *B. napus PURs*. **A** Linear relationship analysis of *B. napus PURs* and the homologous genes in *B. rapa* and *B. oleracea* genomes. **B** Colinear relationship of *PURs* in ZS11. The pie chart represents the percentage of *B. napus PURs* derived from SD, SE, HE, TD, and OR events, respectively; LOSS: Represent the loss of colinear relationship; OR: Represent the allopolyploid event; SE: Represent the segmental exchange event; SD: Represent the segmental duplication event; HE: Represent the homologous exchange event. The blue and orange represent structural genes and *TFs*, respectively. **C** *B. napus PURs* in an An-sub-genome background. Y-axis represents gene numbers, with An-sub-genome background, and X-axis represents duplication events. **D** Selective pressure of *B. napus PURs*. Y-axis represents gene numbers and X-axis represents Ka/Ks values

important role in *B. napus PURs* expansion as well. In addition, six pairs of tandem duplication (TD) genes of *B. napus PURs* were found (Table S4). These results suggested that allopolyploid and small-scale duplication events (especially SD) both contribute to the large expansion of *PURs* in *B. napus*.

We found that all the SE events of *B. napus PURs* were replaced by A_n to C_n subgenome, suggesting that the bias retention of the genes derived from *B. rapa* in *B. napus* after allopolyploid. Furthermore, ~ 93.07% genes (94/101 genes) of *B. napus PURs* that were inherited from *B. rapa* were subsequently duplicated by SD events in *B. napus*, and all the 58 genes that were inherited from C_n-subgenome were replaced by the homologs from A_n-subgenome via HE events (Fig. 2C). This indicated that more genes were inherited from *B. rapa* (74; ~ 94.87%) than from *B. oleracea*, and that more genes from *B. oleracea* genome were replaced by homologs from *B. rapa* genome, suggesting the increasing importance of the *B. rapa* genome background in *B. napus* in P utilization. Additionally, a relatively higher proportion of *TFs* (~ 32.53%, ~ 24.09%) compared to structural genes (~ 25.25%, ~ 18.81%) are derived from allopolyploid and HE events (Fig. 2B), indicating a preferential retention of *TFs* following duplications.

In all, 165 pairs of duplication genes that were generated from small-scale duplication events in *B. napus* (including SD, HE, and TD events) were identified based on the collinearity analysis, including 117 pairs of structural genes, and 48 pairs of *TFs*. The Ka/Ks value of the structural genes (mean ≈ 0.213) and the *TFs* (mean ≈ 0.220) is < 1 by selective pressure analysis, indicating they were under purifying selection (Table S5, Fig. 2D). These results revealed that purifying selection maybe the main evolutionary force for *B. napus PURs*. We further analyzed the sequence identity of the 165 duplicated gene pairs (Table S6). The CDS sequence identity of 95 duplicated gene pairs (~ 57.58%) was ≥ 90%, indicating that they were highly conserved during the evolution. The promoter sequence identity of 105 duplicated gene pairs (~ 63.64%) was ≤ 60%. This result revealed that the promoter regions of duplicated genes had undergone obvious sequence divergence, indicating a differentiation trend among duplication pairs potentially associated with expression and even functional divergence.

Transcriptional regulation profile of *PURs* in *B. napus*

To explore the potential regulatory mechanism of the 285 *B. napus PURs*, we predicted the *cis*-acting regulatory elements (CREs) in the −1,500 bp upstream promoter regions of the candidates. A total of 108 CRE types were obtained, including 29,770 CREs (Table S7). Besides the typical promoter core *cis*-elements (e.g., TATA-box, CAAT-box, and GC-box) and light responsive *cis*-elements, a mass of hormone responsive *cis*-elements, abiotic stress responsive *cis*-elements, and potential TF binding sites were identified (Fig. 3A). Three types of hormone responsive *cis*-elements, namely abscisic acid (ABA) (ABRE; 215 genes), ethylene (ERE; 156 genes), and MeJA (Methyl jasmonate) (TGACG-motif and CGTCA-motif, 192 genes) responsive *cis*-elements were the most ones in promoter regions of *PURs*, suggesting

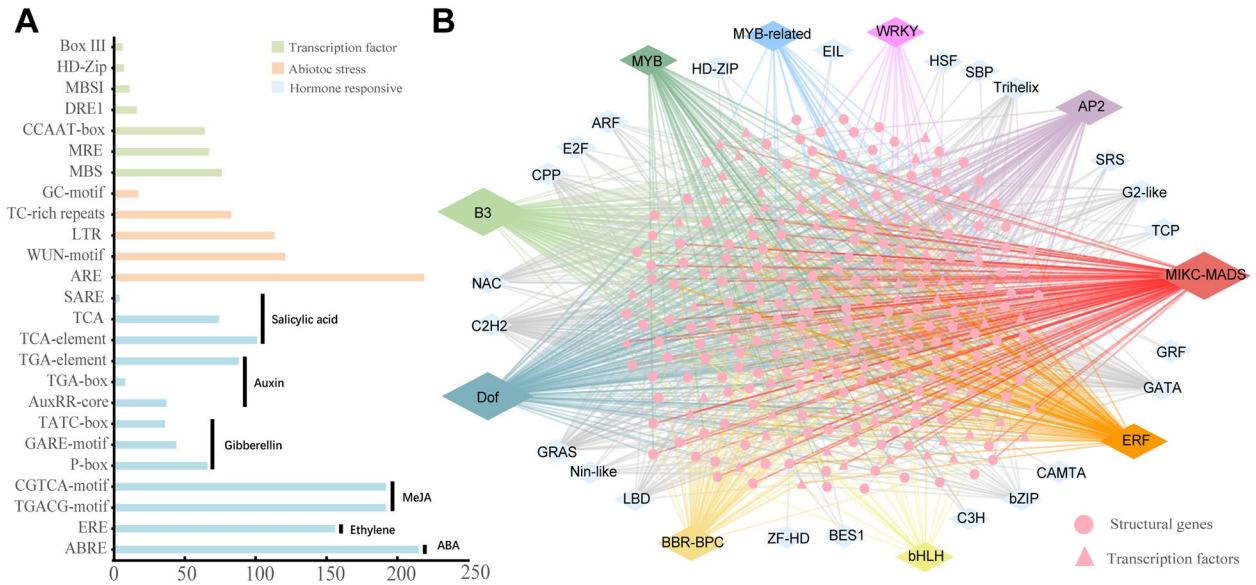

Fig. 3 Transcription and post-transcription regulation analysis of *PURs* in *B. napus*. **A** The 25 types of important CREs in the promoter regions of *PURs*. The X-axis represents the numbers of *PURs*. **B** The potential regulatory interaction between 32 TF families and *PURs*

the potential hormone inducing expression profiles of *PURs* in *B. napus*. The abiotic stress responsive *cis*-elements in the promoters of *PURs* significantly consisted of stress (TC-rich repeats; 83 genes), low temperature and salt stress (DRE1; 16 genes), low temperature (LTR; 113 genes) and wound (WUN-motif, 121 genes) responsive *cis*-elements. Moreover, three major types of potential TF binding sites, including MYB binding site (MBS, 76 genes; MBSI, 11 genes; MRE, 67 genes), HD-Zip3 binding site (HD-Zip 3, 7 genes), Box III binding site (6 genes) were identified in *PURs* promoters. Furthermore, 5,424 potential regulatory relationships between 362 TFs from 32 gene families and *PURs* were predicted by the PlantTFDB database assay (Table S8, Fig. 3B). Excepting for the ZF-HD family that may only regulate one gene, the rest regulate multi-genes respectively, with the members of B3 (98 genes), MIKC_MADS (98 genes) Dof (98 genes), and AP2 (80 genes) families having the largest amount potential regulatory effects on a few *PURs*, exhibiting a hub gene characteristic.

MicroRNA target predictions of *PURs* in *B. napus*

MicroRNAs (miRNAs) play an important role in post-transcriptional gene expression regulation. To explore the potential regulating roles of miRNAs in the Pi utilization gene network, we identified 401 pairs of regulatory relationships among 66 candidate miRNAs targeting 116 of the 285 *B. napus PURs* (Table S9). The candidate miRNAs belonged to 25 families. The number of targeted genes of each miRNA family ranged from 1 to 20 (Fig. 4A), with the majority (21/25, ~ 84.00%) having multi-targets while only a few genes have a single target. One gene could be the target of multiple miRNAs (Fig. 4B), such as *BnaNIGT1.5* and *BnaNIGT1.10* were both targeted by 11 miRNAs (miR164a-d, miR168a, miR395a-f), indicating that different miRNAs acted coordinately in the post-transcriptional regulation process of these *PURs*. In contrast, *BnaNIGT1.2* and *BnaNIGT1.9* were only targeted by miR6029. In addition, a small proportion of miRNA families (8/21, ~ 38.10%) targeted the homologs, while the rest (13/21, ~ 61.90%)) targeted different types of genes. For instance, miR169 targeted six homologs in the PHT1 family (*BnaPHT1.1*, *BnaPHT1.16*, *BnaPHT1.27*, *BnaPHT1.29*, *BnPHT1.6* and *BnaPHT1.7*), while miR164a-d may target different types of genes (*BnaTPT1*, *BnaCK2.33*, *BnaALIX2*, *BnaNIGT1.5*, and *BnaNIGT1.10*) encoding TFs, plastic Pi translocator, phosphorylation and Pi transporter degradation, implicating the complicated expression profile and function of *PURs*.

Spatiotemporal expression profile of *PURs* in *B. napus*

Gene expression profile is generally associated with its function. To investigate the spatiotemporal transcripts of *B. napus PURs*, we used transcriptome data from 90

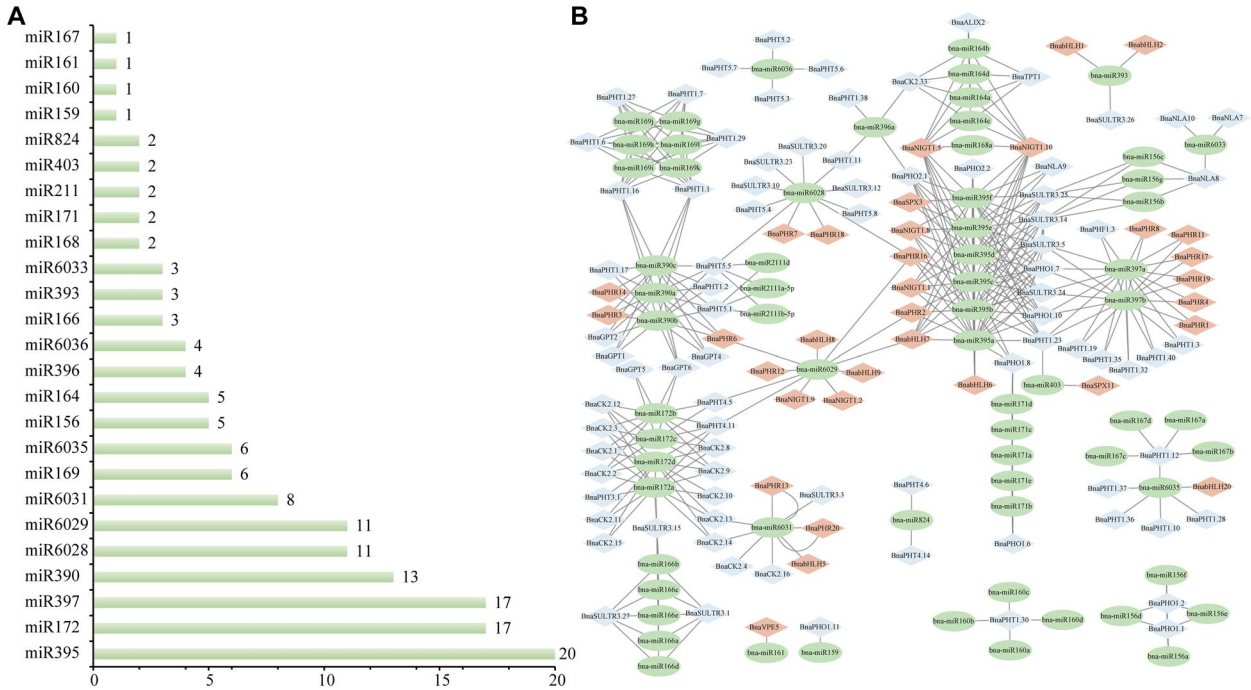

Fig. 4 MicroRNAs predictions of *PURs* in *B. napus*. **A** The 25 type miRNA families of *PURs*. The X-axis represent the targeted gene numbers. **B** The potential miRNA regulatory relationships between *PURs*. Green ovals represent miRNAs, blue rhombuses represent structural genes and pink rhombuses represent *TFs*

ZS11 samples at various developmental stages in BnIR (https://yanglab.hzau.edu.cn/BnIR).

The results showed that 238 of the 285 *PURs* (~83.51%) had detectable transcript levels (FPKM ≥ 1) in at least one investigated organ or tissue, including a total of 77 *TFs* and 161 structural genes (Table S10, Figure S2). The last (47 genes) had weak (FPKM < 1) or no detectable expression value in the samples, and thus were excluded. For the structural genes, relatively fewer genes had high expression levels in reproductive organs, while most of them were preferentially expressed in vegetative organs, such as silique wall (96 genes) and roots (91 genes) (Fig. 5A). The same trend was observed for *TFs*, indicating a close relationship between these two gene types and highlighting the higher Pi requirement of vegetative organs compared to reproductive organs. Moreover, we found that ~76.42% (94) duplicated gene pairs shared conserved expression pattern (|Pearson correlation coefficient| ≥ 0.6), while ~23.58% (29) of them exhibited different expression patterns (|Pearson

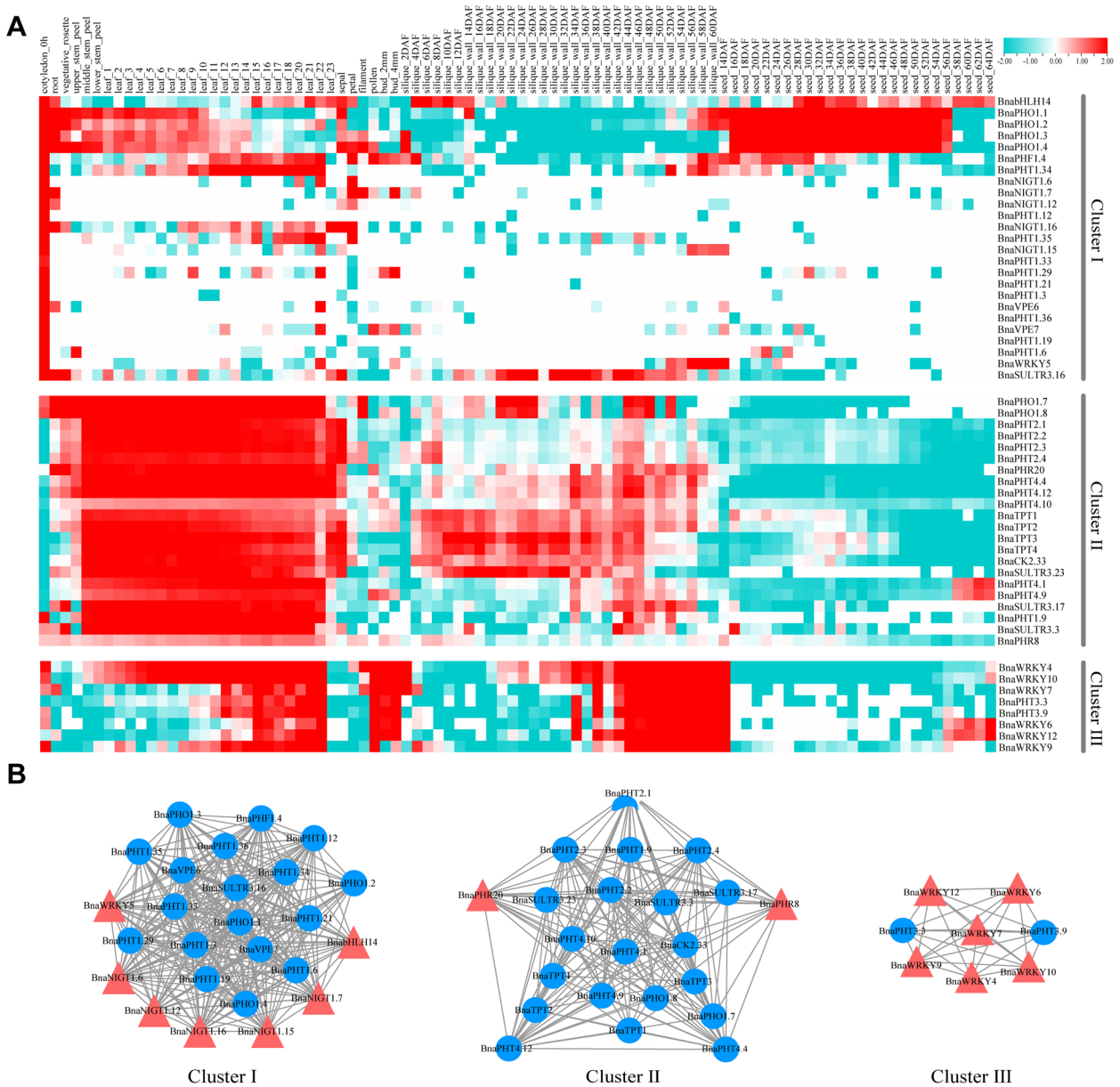

Fig. 5 The three major clusters (I to III) of the Spatiotemporal co-expression gene network in *B. napus PURs*. **A** depicts the spatiotemporal expression profile of *PURs* and **B** depicts the corresponding gene network from each cluster. The *PURs* with no or weak expression levels (FPKM < 1) were removed from the heatmap. The color bar at the low right represents log2 expression value (FPKM ≥ 1): green represents low expression, and red represents high expression

correlation coefficient|< 0.6) (Table S6). This result suggested that the majority of duplicated gene pairs exhibited functional redundancy, with some duplicated genes undergoing expression divergence and even functional differentiation.

A total of 828 co-expression relationship pairs (|Pearson value|≥ 0.6; *p*-value ≤ 0.01) of *PURs* were identified by co-expression analysis, forming a complex gene network that was further divided into three groups (I-III) (Figure S3). Group I consisted of 25 genes, including 18 structural genes and 7 *TFs*, which were highly expressed in cotyledon. Group II contained 20 structural genes and 2 *TFs*, with most of them (16 genes) being highly expressed in leaves (FPKM ≥ 20) and/or in silique wall tissues (13 genes), which were mainly involved in Pi uptake and transport processes. Group III contained 2 structural genes and 6 *TFs*, which were highly expressed in mature leaf, bud, and silique tissues (Fig. 5B). These results indicated that *PURs* may play wide roles during the entire growth period of *B. napus* in a temporal and spatial pattern. Moreover, we identified 10 potential hub genes based on the co-expression relationship (Figure S4), including *BnaPHT1.12*, *BnaPHT1.16*, *BnaPHT1.36*, *BnaPHT1.19*, *BnaPHT1.21*, *BnaPHT1.33*, *BnaPHT1.3*, *BnaPHT1.4*, *BnaPHT1.6*, and *BnaNIGT1.12*.

Low Pi stress expression profile of *PURs* in *B. napus*

To assess the potential role of *PURs* in low Pi stress response processes in *B. napus*, we analyzed the expression profiles of candidates using the ZS11 low Pi stress RNA-seq dataset in BnGADB (http://www.BnaGADB.cn/).

As many as 223 of the 285 genes (78.25%) had detectable transcript levels (FPKM ≥ 1) in *B. napus* root or leaf tissues under LP conditions, including 73 *TFs* and 150 structural genes (Table S11, Figure S5). Among them, four genes (*BnaNIGT1.3*, *BnaPHT1.26*, *BnaPHT4.15*, and *BnaSULTR3.27*) that were not expressed under normal conditions displayed detectable expression levels in the LP RNA-seq dataset, suggesting a low Pi stress inducible expression profile. The expressions of *PURs* were either preferentially and even specially expressed in roots or leaves respectively, showing a temporal and spatial expression trend. Moreover, 90 of the 233 (~ 38.63%) genes were identified as differentially expressed genes (DEG, log2FoldChange > 2) under low Pi treatment. Among them, 49, 57, and 79 genes were differentially expressed at 5, 7, and 12 days under low Pi treatments in roots and/or leaves, displaying a delayed LP induced expression trend. Meanwhile, some genes were continuously expressed (37 genes) or continuously differentially expressed (7 genes) in roots or leaves, such as *BnaPHO1.8*, *BnaSPX3*, and *BnaNIGT1.8*, suggesting their potential functional characteristic in *B. napus* (Table S12). These results illustrated that *PURs* were sensitive to Pi starvation in roots or leaves.

Co-expression analysis identified 2021 co-expression relationship pairs (|Pearson value|≥ 0.6; *p*-value ≤ 0.01) of *PURs* in the low Pi stress dataset, which was further divided into three groups (I-III) (Figure S6). Group I included 27 structural genes which were consistently highly expressed in leaves. Group II was composed of 24 structural genes and 8 *TFs*, which were highly expressed in roots. Group III contained 15 structural genes and 11 *TFs*, which were highly expressed in roots as well (Fig. 6A). Moreover, we identified 10 potential hub genes based on the co-expression relationship (Fig. 6B, Figure S4), namely *BnaPHT2.1*, *BnaPHT2.2*, *BnaPHT2.3*, *BnaPHT2.4*, *BnaPHT4.4*, *BnaPHT4.5*, *BnaPHT4.11*, *BnaPHT4.12*, *BnaCK2.33*, and *BnaSULTR3.23* gene.

Comparative expression profiles of candidate *PURs* in different *B. napus* varieties

In our previous study, we investigated the root system architecture for 370 *B. napus* germplasms under LP condition [29]. Based on the DEGs and co-expression analysis of the LP RNA-seq dataset (Table S11, S12, Fig. S6), four DEGs from *PHT1* (*BnaPHT1.7* and *BnaPHT1.9*) and *SPX* (*BnaSPX6* and *BnaSPX7*) families which represented the structural genes and regulatory genes as well as the central nodes in the LP co-expression network were selected to further analyze their application potential roles in response to LP stress by qRT-PCR assay in three germplasms ("226", "252" and "470"). Among them, "226" represents the control group (ZS11), while "252" and "470" represent the groups with undeveloped and developed RSA traits under low Pi supply respectively [29] (Fig. 7A). From the LP RNA-seq dataset in "ZS11", the log2 fold changes (FC) for *SPX6* at 5, 7, and 12 days were 1.75, 2.42, and 2.28, respectively; for *SPX7*, they were 0.48, 2.29, and 5.34, respectively; for *PHT1.7*, they were 2.15, 3.13, and 3.28, respectively; and for *PHT1.9*, they were 0.83, 1.70, and 1.60, respectively. Similar to our RNA-seq analysis, all of the four genes were generally induced by low Pi treatments. However, a distinct response pattern was found between "226/470" and "252" (Fig. 7B). The expressions of the four genes were up-regulated in "226" and "470" while were down-regulated in "252" under LP condition. Moreover, all of the four genes showed a significant up-regulated expression from 4 to 12d in "470". The close positive relationship between the expression levels of the four genes and the RSA traits of the three *B. napus* germplasms under LP conditions demonstrated the important roles of these *PURs* in responding to low Pi stress in *B. napus*.

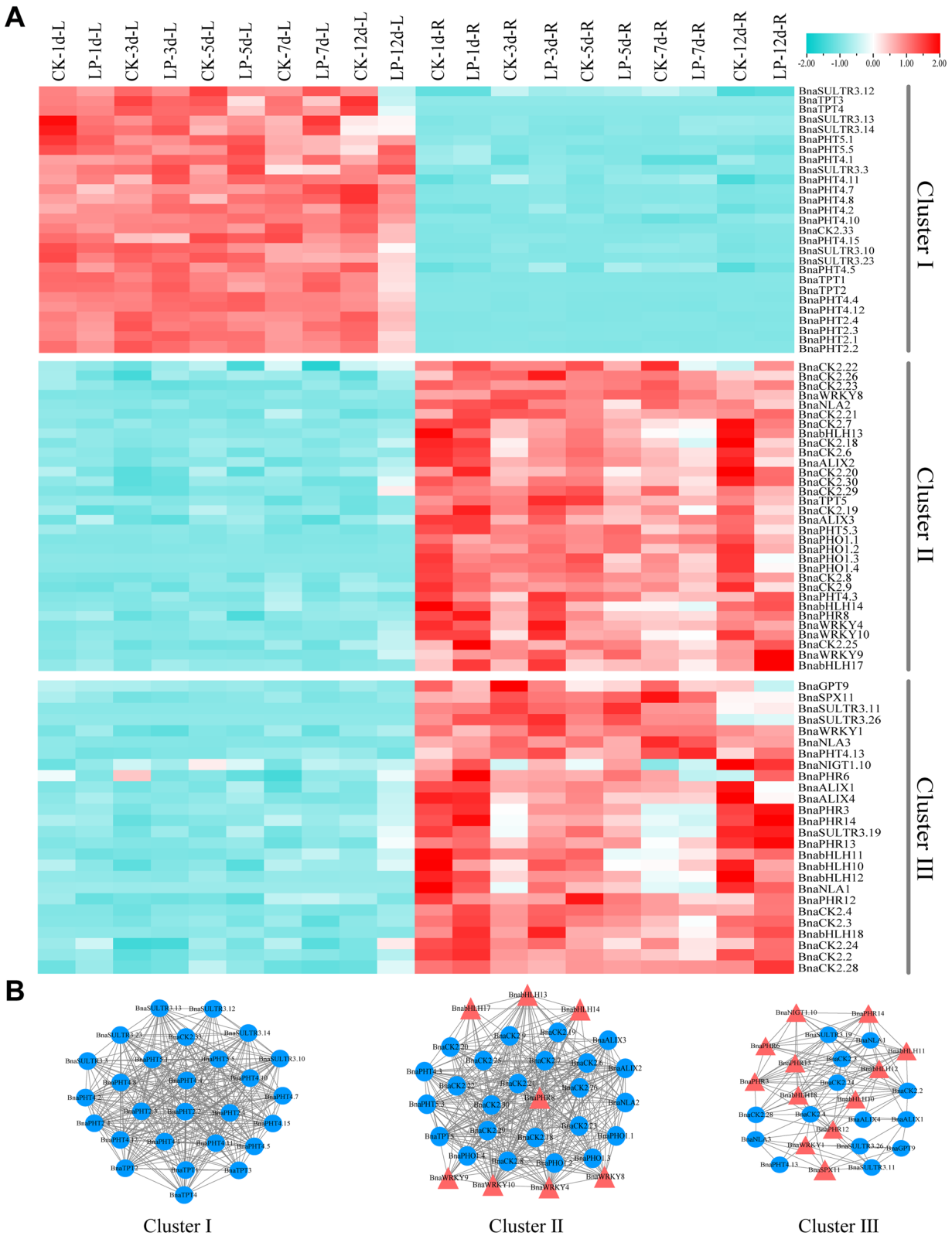

Fig. 6 The three major clusters (I to III) of the low Pi stress co-expression gene network in *B. napus PURs*. **A** depicts the low Pi stress expression profile of *PURs* and **B** depicts the corresponding gene network from each cluster. "d" indicates the day after low Pi treatment; "L" represents leaf sample; "R" represents root sample. The *PURs* with no or weak expression levels (FPKM < 1) were removed from the heatmap. The color bar at the low right represents log2 expression value (FPKM ≥ 1): green represents low expression, and red represents high expression

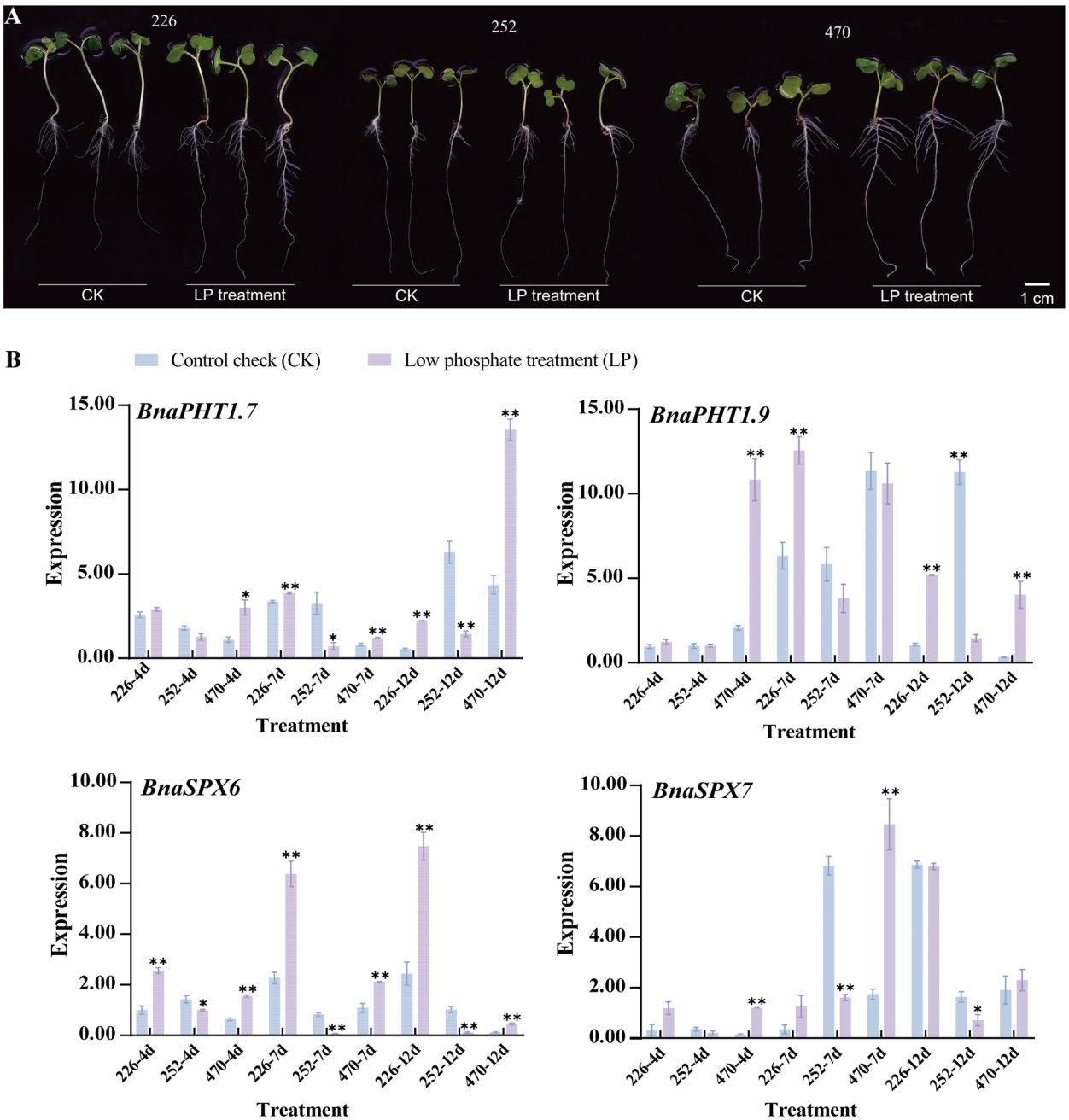

Fig. 7 Comparative expression profiles of candidate *PURs* in different *B. napus* varieties. **A** RSA of 3 *B. napus* varieties on control check (CK) and low Pi treatment (LP) in 7d. **B** Expressions of four genes in *PURs* under low Pi treatments by qRT-PCR. The transcript levels were investigated in *B. napus* seedling roots under LP conditions by qRT-PCR method. CK: normal P condition; LP: low Pi treatment. d: day (s) after low Pi treatment. Error bars indicate the standard deviation of three independent experiments. "*" indicates significant difference ($0.05 > p > 0.01$); "**" indicates extremely significant difference ($p < 0.01$)

Discussion

Small-scale duplication events play an important role in *PURs* expansion

Whole genome duplication (WGD) and small-scale duplications (SSD) were the major driving forces for the evolution and diversification of land plants, which provide rich evolutionary resources for species and contribute to the promotion of environmental adaptability [30–35]. After multiple rounds of WGD/SSD, plant genomes contain a large number of duplicated

genes, forming a mass of gene families [30, 31]. Therefore, WGD and SSD are recognized as the major driving forces for gene expansion in plants during their evolution.

In most cases, WGD events contributed more to gene expansion than SSD events in angiosperms. For example, WGD was demonstrated to be the predominant driving force for the expansion of P450, T6P, and WAK gene families in *Arabidopsis* [36–38], and VQ, AGC, and CSN families in rice [39–41]. We also proved that WGD mainly contributed to the large expansion of MADS, bHLH, and TCP families in *B. napus* [40–44]. SSD event was widely reported to play a major role in plant gene expansion as well. For instance, segmental duplication accounted for the rapid expansion and large size of *PHB* gene expansion in *Arabidopsis* [45], *IQM* genes in rice [46], CPK and RBL gene families in wheat [47, 48], and the R2R3-MYB gene family in land plants [49]. Moreover, WGD is often followed by the loss of most duplicated genes over a few million years [50], whereas various types of SSD occur more or less continuously and are essential in plant development and adaptation to the environment [51, 52]. Many studies found that the expansion of genes related to signal transduction, transcriptional regulation, and ribosome structures were mainly driven by WGD events [53, 54], while those related to environmental stress responses were mainly driven by SSD events [55, 56]. Accordingly, plants have produced a series of Pi starvation adaptation features by amplifying and retaining genes related to Pi acquisition, transport, and signal transduction, after long-term evolution [2].

In this study, we found a higher proportion of SSD events (179 genes) occurred during the expansion of *PURs* than that of the WGD events (78 genes) in *B. napus*. Moreover, most DEGs of *B. napus PURs* under low Pi treatments were from SSD events (64/90), especially from SD events (34/90). These results demonstrated that the expansion and retention bias of the *PURs* derived from SSD events that were involved in low Pi stress response. Furthermore, we found that more *PURs* were inherited from *B. rapa* than from *B. oleracea*, and more *PURs* from the *B. oleracea* genome were replaced by the homologs from the *B. rapa* genome. This suggested the predominant *B. napus* background of the P utilization feature in *B. napus* during the evolution.

Expression analysis implied the potential roles of *PURs* in response to low Pi stress *in B. napus*

P is one of the most important yet frequently deficient macronutrients in plants, thereby its availability is crucial for crop production [1]. When Pi availability is limited in soil, plants can undergo a range of adaptation mechanisms to Pi stress response either to acquire more Pi from the environment and/or to remobilize Pi within the plant body to maintain Pi homeostasis, such as changes in the RSA, alteration of Pi allocation between shoots and roots, increasing in Pi uptake/transport/remobilization [57–59]. Most of these developmental, physiological, and biochemical processes depend on triggering the expressions of *PURs* [58, 60]. To date, many *PURs* have been identified and functionally characterized in *Arabidopsis* and rice, and their regulatory networks were well elucidated [6–8, 17, 61], forming a complex gene network for the Pi utilization process in plants. However, little is known about *PURs* in most crops, such as *B. napus*. In this study, we obtained 285 candidate *PURs* by systematic bioinformatic identification in *B. napus* genome at a genome-wide level, providing a valuable gene resource for further function research.

Gene expression patterns can provide important clues for its function [62]. Many studies have shown that *PURs* widely respond to Pi condition in the environment [58–60]. For example, *Arabidopsis AtPHT1;1* and *AtPHT1;4* genes which exhibited the highest transcript levels in roots acted as the major Pi transporter in roots under LP conditions [5, 6]; rice *OsPHT1;2* that was abundantly expressed in roots and was highly induced by Pi deficiency, played a critical role in Pi transportation from roots to shoots [63]; *PHO1* and its homolog (e.g., *MtPHO1.1/1.2* in *Medicago truncatula* [64], *CaPHO1s* in *Cicer arietinum* [65], *OsPHO1;2* in rice [66]) were induced by low Pi treatments in roots, and played a key role in Pi transport from roots to shoots [8]. Similar to the structural genes, many *TFs* involved in Pi utilization were widely demonstrated to have a Pi level-induced gene expression which then regulated the transcriptions of *PURs* directly or indirectly [11, 12, 14, 58]. For example, the expression of *Arabidopsis WRKY45* was prominently induced in roots under Pi starvation situation, which then activated *AtPHT1;1* expression in response to Pi starvation [12]; *Arabidopsis AtPHR1* and its *AtPHL* homologs was the well-known master regulator for Pi starvation responses by regulating many *PURs*, such as *PHO1*, *PGT1*, *PHF1* [67, 68]; *AtSPX1-4* genes of the SPX family were induced/reduced to different extents, and then acted as regulators for the transcriptional activity of *PHR1* [13, 14, 61, 69]; whereas GARP family member, *NIGT1*, modulate Pi uptake and starvation signaling by regulating the expressions of SPX genes [70, 71].

Similarly, in the present study, our LP RNA-seq data showed that most homologs of candidate *PURs* including structural genes and *TFs* (~38.63%) were strongly induced under LP conditions in *B. napus* (Table S12). For instance,

BnaPHT1.4, *BnaPHT1.7*, *BnaPHT1.29*, *BnaPHT3.10*, *BnaNIGT1.13*, *BnaNIGT1.3*, *BnaNIGT1.8*, *BnaPHO1.5*, *BnaPHO1.10*, *BnaSPX7* and *BnaSPX8* were significantly up-regulated in *B. napus* roots under LP condition; while *BnaPHF1.1*, *BnaPHF1.2*, *BnaPHF1.4*, *BnaPHO1.5*, *BnaPHO1.7*, *BnaPHO1.10*, *BnaSULTR3.9*, *BnaPHT1.40*, *BnaSPX1*, *BnaSPX2*, *BnaSPX9* and *BnaSPX10* were significantly up-regulated in leaves under low Pi stress. These results suggested that the LP inducible *PURs* in *B. napus* may contribute to low Pi stress response. Based on our results (Figs. 6, 7) and reported research, *BnaPHT1.9* and *BnaPHT1.7* are likely to function as primary phosphate transporters, particularly under phosphorus-deficient conditions, facilitating uptake and redistribution of phosphate [5, 6, 63]. *BnaSPX6* and *BnaSPX7* may act as regulatory components in phosphate signaling pathways, consistent with the known functions of *SPX* family proteins [13, 14, 61, 69]. These predictions provide valuable insights into the molecular mechanisms underlying phosphate homeostasis and offer a basis for further experimental investigations.

Conclusions

In this study, 285 *PURs* were identified from 21 gene families in *B. napus* genome. The *PURs* were widely distributed in plant kingdom with a rapid expansion trend. The allopolyploid event between its ancestors and the SSD events in *B. napus* are both the main driving forces for *PURs* expansion. More *PURs* that were inherited from *B. rapa* exhibited a wide expression profile during the whole growth period of *B. napus*. Most *B. napus PURs* exhibited strong low Pi stress inducible expression profile. *BnaPHT1.9*, *BnaPHT1.7*, *BnaSPX6*, and *BnaSPX7* showed significantly up-regulated expression profiles in root-developed varieties while down-regulated expression levels in root-undeveloped varieties under LP condition, indicating their potential roles in *B. napus*. Overall, this study provides important clues about the potential functions of *PURs* that may hold significant value in enhancing *B. napus* PUE and cultivating new varieties.

Supplementary Information

The online version contains supplementary material available at https://doi.org/10.1186/s12870-025-06315-1.

Additional file 1: Table S1. Primer list of the genes for qRT-PCR analysis in this study.

Additional file 2: Table S2. Information of Phosphate (Pi) utilization related genes (*PURs*) in *Brassica napus* identified in this study.

Additional file 3: Table S3. Gene list of *PURs* in 34 plant species identified in this study.

Additional file 4: Table S4. Duplications of *PURs* in *B. napus*.

Additional file 5: Table S5. The Ka/Ks values of duplication gene pairs in *PURs* in *B. napus*.

Additional file 6: Table S6. Pearson correlation coefficient of duplication gene pairs of *PURs* in *B. napus*.

Additional file 7: Table S7. *Cis*-acting regulatory elements of *PURs* in *B. napus*.

Additional file 8: Table S8. Transcription factor (TF) binding sites in the promoter regions of *PURs* in *B. napus*.

Additional file 9: Table S9. Prediction of microRNA targets in *PURs* in *B. napus*.

Additional file 10: Table S10. Spatiotemporal expression profiles of *PURs* in *B. napus*.

Additional file 11: Table S11. Low Pi stress expression profiles of *PURs* in *B. napus*.

Additional file 12: Table S12. Differentially expressed genes of *PURs* in the low Pi stress dataset in *B. napus*.

Additional file 13: Figure S1. Chromosome location of *PURs* in *B. napus*. The blue and orange represent structural genes and *TFs*, respectively. Figure S2. Tissue expression profile of *PURs* in *B. napus*. The *PURs* with no or weak expression levels (FPKM < 1) were removed from the heatmap. The color bar at the low right represents log2 expression value (FPKM ≥ 1): green represents low expression, and red represents high expression. Figure S3. Gene co-expression network of the spatiotemporal expression profile of *PURs* in *B. napus*. The red triangles represent transcription factors, and the blue circles represent structural genes. Figure S4. Expression patterns of core genes in co-expression networks of *PURs* in *B. napus*. (A) Spatiotemporal expression patterns of core genes in co-expression network of *PURs* in *B. napus*. (B) Expression patterns of core genes in co-expression network of *PURs* under low Pi stress in *B. napus*. Figure S5. Low Pi stress expression profile of *PURs* in *B. napus*. Figure S6. Gene co-expression network of low Pi stress expression profile of *PURs* in *B. napus*. The red triangles represent transcription factors, and the blue circles represent structural genes.

Acknowledgements
Not applicable.

Authors' contributions
H.D: supervised and designed the experiments; Y.B.S and J.Q.C: drafted and revised the manuscript. H.J.L, W.Y.Z, Z.C, R.J.D, Z.X.W, S.Y.L, L.Z, S.N.Z: data analysis. F.M.Y, N.W.Y, H.Y.Z, J.N.L, and C.M.Q: critically edited the manuscript. All authors have reviewed and agreed to the final version of the manuscript.

Funding
This work was supported by the National Key Research and Development Program of China (2023YFF1000701), the 2024 Key Core Agricultural Technologies R&D Program of Chongqing: Development and Application of Short-Cycle Rapeseed Germplasm Resources, and the Natural Science Foundation of Chongqing, China (CSTB2022NSCQ-MSX0790).

Data availability
Availability of data and materials data are provided within the manuscript and supplementary information files.

Declarations

Ethics approval and consent to participate
Not applicable.

Consent for publication
Not applicable.

Competing interests
The authors declare no competing interests.

Author details
[1]College of Agronomy and Biotechnology, Chongqing Engineering Research Center for Rapeseed, Southwest University, Chongqing 400716, China. [2]Academy of Agricultural Sciences, Southwest University, Chongqing 400716, China.

Received: 6 June 2024 Accepted: 27 February 2025
Published online: 13 March 2025

References

1. Brinch-Pedersen H, Sørensen LD, Holm PB. Engineering crop plants: getting a handle on phosphate. Trends Plant Sci. 2002;7(3):118–25. https://doi.org/10.1016/s1360-1385(01)02222-1.
2. Rouached H, Arpat AB, Poirier Y. Regulation of Phosphate Starvation Responses in Plants: Signaling Players and Cross-Talks. Mol Plant. 2010;3(2):288–99. https://doi.org/10.1093/mp/ssp120.
3. Raghothama KG. Phosphate Acquisition. Annu Rev Plant Physiol Plant Mol Biol. 1999;50(1):665–93. https://doi.org/10.1146/annurev.arplant.50.1.665.
4. Gilbert GA, Knight JD, Vance CP, Allan DL. Acid phosphatase activity in phosphorus-deficient white lupin roots. Plant Cell Environ. 2002;22(7):801–10. https://doi.org/10.1046/j.1365-3040.1999.00441.x.
5. Rausch C, Bucher M. Molecular mechanisms of phosphate transport in plants. Planta. 2002;216(1):23–37. https://doi.org/10.1007/s00425-002-0921-3.
6. Shin H, Shin HS, Dewbre GR, Harrison MJ. Phosphate transport in *Arabidopsis*: Pht1;1 and Pht1;4 play a major role in phosphate acquisition from both low- and high-phosphate environments. Plant J. 2004;39(4):629–42. https://doi.org/10.1111/j.1365-313X.2004.02161.x.
7. Wang D, Lv S, Jiang P, Li Y. Roles, Regulation, and Agricultural Application of Plant Phosphate Transporters. Front Plant Sci. 2017;8. https://doi.org/10.3389/fpls.2017.00817.
8. Hamburger D, Rezzonico E, Petétot JMC, Somerville C, Poirier Y. Identification and characterization of the *Arabidopsis* gene involved in phosphate loading to the xylem. Plant Cell. 2002;14(4):889–902. https://doi.org/10.1105/tpc.000745.
9. Versaw WK, Garcia LR. Intracellular transport and compartmentation of phosphate in plants. Curr Opin Plant Biol. 2017;39:25–30. https://doi.org/10.1016/j.pbi.2017.04.015.
10. Yang SY, Huang TK, Kuo HF, Chiou TJ. Role of vacuoles in phosphorus storage and remobilization. J Exp Bot. 2017;68(12):3045–55. https://doi.org/10.1093/jxb/erw481.
11. Rubio V, Linhares F, Solano R, Martín AC, Iglesias J, Leyva A, Paz-Ares J. A conserved MYB transcription factor involved in phosphate starvation signaling both in vascular plants and in unicellular algae. Genes Dev. 2001;15(16):2122–33. https://doi.org/10.1101/gad.204401.
12. Wang H, Xu Q, Kong Y-H, Chen Y, Duan J-Y, Wu W-H, Chen Y-F. *Arabidopsis* WRKY45 Transcription Factor Activates PHOSPHATE TRANSPORTER1;1 Expression in Response to Phosphate Starvation. Plant Physiol. 2014;164(4):2020–9. https://doi.org/10.1104/pp.113.235077.
13. Liu F, Wang ZY, Ren HY, Shen CJ, Li Y, Ling HQ, Wu CY, Lian XM, Wu P. OsSPX1 suppresses the function of OsPHR2 in the regulation of expression of and phosphate homeostasis in shoots of rice. Plant J. 2010;62(3):508–17. https://doi.org/10.1111/j.1365-313X.2010.04170.x.
14. Lv QD, Zhong YJ, Wang YG, Zhang L, Shi J, Wu ZC, Liu Y, Mao CZ, Yi KK, Wu P. SPX4 Negatively Regulates Phosphate Signaling and Homeostasis through Its Interaction with PHR2 in Rice. Plant Cell. 2014;26(4):1586–97. https://doi.org/10.1105/tpc.114.123208.
15. Chiou TJ, Aung K, Lin SI, Wu CC, Chiang SF, Su CL. Regulation of phosphate homeostasis by microRNA in *Arabidopsis*. Plant Cell. 2006;18(2):412–21. https://doi.org/10.1105/tpc.105.038943.
16. Lei KJ, Lin YM, Ren J, Bai L, Miao YC, An GY, Song CP. Modulation of the Phosphate-Deficient Responses by microRNA156 and its Targeted SQUAMOSA PROMOTER BINDING PROTEIN-LIKE 3 in *Arabidopsis*. Plant Cell Physiol. 2016;57(1):192–203. https://doi.org/10.1093/pcp/pcv197.
17. González E, Solano R, Rubio V, Leyva A, Paz-Ares J. Phosphate transporter traffic facilitator1 is a Plant-Specific SEC12-Related Protein That Enables the Endoplasmic Reticulum Exit of a High-Affinity Phosphate Transporter in *Arabidopsis* [W]. Plant Cell. 2005;17(12):3500–12. https://doi.org/10.1105/tpc.105.036640.
18. Sega P, Kruszka K, Szweykowska-Kulinska Z, Pacak A. Identification of transcription factors that bind to the 5′-UTR of the barley *PHO2* gene. Plant Mol Biol. 2020;102(1–2):73–88. https://doi.org/10.1007/s11103-019-00932-9.
19. Liu T-Y, Huang T-K, Tseng C-Y, Lai Y-S, Lin S-I, Lin W-Y, Chen J-W, Chiou T-J. PHO2-Dependent Degradation of PHO1 Modulates Phosphate Homeostasis in *Arabidopsis*. Plant Cell. 2012;24(5):2168–83. https://doi.org/10.1105/tpc.112.096636.
20. Park BS, Seo JS, Chua NH. Nitrogen Limitation Adaptation Recruits PHOSPHATE2 to Target the Phosphate Transporter PT2 for Degradation during the Regulation of Phosphate Homeostasis. Plant Cell. 2014;26(1):454–64. https://doi.org/10.1105/tpc.113.120311.
21. Pacak A, Barciszewska-Pacak M, Swida-Barteczka A, Kruszka K, Sega P, Milanowska K, Jakobsen I, Jarmolowski A, Szweykowska-Kulinska Z. Heat Stress Affects Pi-related Genes Expression and Inorganic Phosphate Deposition/Accumulation in Barley. Front Plant Sci. 2016;7. https://doi.org/10.3389/fpls.2016.00926.
22. Bari R, Pant BD, Stitt M, Scheible WR. PHO2, microRNA399, and PHR1 define a phosphate-signaling pathway in plants. Plant Physiol. 2006;141(3):988–99. https://doi.org/10.1104/pp.106.079707.
23. Song JM, Guan ZL, Hu JL et al. Eight high-quality genomes reveal pan-genome architecture and ecotype differentiation of *Brassica napus*. Nature Plants. 2020; 6(1):34-+. https://doi.org/10.1038/s41477-019-0577-7.
24. Chalhoub B, Denoeud F, Liu S, et al. Early allopolyploid evolution in the post-Neolithic Brassica napus oilseed genome. Science. 2014;345(6199):950–3. https://doi.org/10.1126/science.1253435.
25. Wolfgang Friedt JT, Tingdong Fu. Academic and Economic Importance of *Brassica napus* Rapeseed. The Brassica napus Genome. 2018;1–20. https://doi.org/10.1007/978-3-319-43694-4.
26. Li P, Wen J, Chen P, Guo P, Ke Y, Wang M, Liu M, Tran L-SP, Li J, Du H. MYB Superfamily in Brassica napus: Evidence for Hormone-Mediated Expression Profiles, Large Expansion, and Functions in Root Hair Development. Biomolecules. 2020;10(6):875. https://doi.org/10.3390/biom10060875.
27. Wang DP, Zhang YB, Zhang Z, Zhu J, Yu J. KaKs_Calculator 2.0: a toolkit incorporating gamma-series methods and sliding window strategies. Genomics Proteomics Bioinformatics. 2010;8(1):77–80. https://doi.org/10.1016/S1672-0229(10)60008-3.
28. Shannon P, Markiel A, Ozier O, Baliga NS, Wang JT, Ramage D, Amin N, Schwikowski B, Ideker T. Cytoscape: a software environment for integrated models of biomolecular interaction networks. Genome Res. 2003;13(11):2498–504. https://https://doi.org/10.1101/gr.1239303.
29. Yuan P, Liu HJ, Wang XH, Hammond JP, Shi L. Genome-wide association study reveals candidate genes controlling root system architecture under low phosphorus supply at seedling stage in *Brassica napus*. Molecular Breeding. 2023;43(8). https://doi.org/10.1007/s11032-023-01411-2.
30. Jiao YN, Wickett NJ, Ayyampalayam S, et al. Ancestral polyploidy in seed plants and angiosperms. Nature. 2011;473(7345):97–U113. https://doi.org/10.1038/nature09916.
31. Panchy N, Lehti-Shiu M, Shiu SH. Evolution of Gene Duplication in Plants. Plant Physiol. 2016;171(4):2294–316. https://doi.org/10.1104/pp.16.00523.
32. Landis JB, Soltis DE, Li Z, Marx HE, Barker MS, Tank DC, Soltis PS. Impact of whole-genome duplication events on diversification rates in angiosperms. Am J Bot. 2018;105(3):348–63. https://doi.org/10.1002/ajb2.1060.
33. Oh DH, Dassanayake M. Landscape of gene transposition-duplication within the Brassicaceae family. DNA Res. 2019;26(1):21–36. https://doi.org/10.1093/dnares/dsy035.
34. Wu S, Han B, Jiao Y. Genetic Contribution of Paleopolyploidy to Adaptive Evolution in Angiosperms. Mol Plant. 2020;13(1):59–71. https://doi.org/10.1016/j.molp.2019.10.012.
35. Hu TT, Pattyn P, Bakker EG, Cao J, Cheng JF, Clark RM, Fahlgren N, Fawcett JA, Grimwood J, Gundlach H et al: The genome sequence and the basis of rapid genome size change. Nature Genetics. 2011;43(5):476-+. https://doi.org/10.1038/ng.807.
36. Yu JY, Tehrim SH, Wang L, Dossa K, Zhang XR, Ke T, Liao BS. Evolutionary history and functional divergence of the cytochrome P450 gene superfamily between and species uncover effects of whole genome and tandem duplications. Bmc Genomics. 2017;18(1). https://doi.org/10.1186/s12864-017-4094-7.
37. Vandesteene L, López-Galvis L, Vanneste K, et al. Expansive Evolution of the TREHALOSE-6-PHOSPHATE PHOSPHATASE Gene Family in *Arabidopsis*. Plant Physiol. 2012;160(2):884–96. https://doi.org/10.1104/pp.112.201400.
38. Zhang ZQ, Huo WQ, Wang XX, et al. Origin, evolution, and diversification of the wall-associated kinase gene family in plants. Plant Cell Rep. 2023;42(12):1891–906. https://doi.org/10.1007/s00299-023-03068-9.

39. Ma JF, Wang RB, Zhao HY, et al. Genome-wide characterization of the VQ genes in Triticeae and their functionalization driven by polyploidization and gene duplication events in wheat. Int J Biol Macromolecules. 2023;243. https://doi.org/10.1016/j.ijbiomac.2023.125264.
40. Jiang YF, Liu XH, Zhou MG, Yang J, Ke SM, Li YS. Genome-Wide Identification of the AGC Protein Kinase Gene Family Related to Photosynthesis in Rice. Int J Mol Sci. 2022;23(20). https://doi.org/10.3390/ijms232012557.
41. Shi B, Hou J, Yang J, Han I-J, Tu D, Ye S, Yu J, Li L. Genome-wide analysis of the CSN genes in land plants and their expression under various abiotic stress and phytohormone conditions in rice. Gene. 2023;850. https://doi.org/10.1016/j.gene.2022.146905.
42. Wu YW, Ke YZ, Wen J, Guo PC, Ran F, Wang MM, Liu MM, Li PF, Li JN, Du H. Evolution and expression analyses of the MADS-box gene family in *Brassica napus*. Plos One. 2018;13(7). https://doi.org/10.1371/journal.pone.0200762.
43. Ke YZ, Wu YW, Zhou HJ, Chen P, Wang MM, Liu MM, Li PF, Yang J, Li JN, Du H. Genome-wide survey of the bHLH super gene family in *Brassica napus*. Bmc Plant Biology. 2020;20(1). https://doi.org/10.1186/s12870-020-2315-8.
44. Liu MM, Wang MM, Yang J, Wen J, Guo PC, Wu YW, Ke YZ, Li PF, Li JN, Du H. Evolutionary and Comparative Expression Analyses of TCP Transcription Factor Gene Family in Land Plants. Int J Mol Sci. 2019;20(14). https://doi.org/10.3390/ijms20143591.
45. Di C, Xu WY, Su Z, Yuan JS. Comparative genome analysis of PHB gene family reveals deep evolutionary origins and diverse gene function. Bmc Bioinformatics. 2010;11(S6). https://doi.org/10.1186/1471-2105-11-S6-S22.
46. Fan T, Lv TX, Xie CP, Zhou YP, Tian CG. Genome-Wide Analysis of the Gene Family in Rice (*Oryza sativa* L.). Plants-Basel. 2021;10(9). https://doi.org/10.3390/plants10091949.
47. Liu ML, Wang CC, Xu Q, Jiang BL, Zhang LT, Zhang Y, Tian ZB, Chang C, Zhang HP. Genome-wide identification of the CPK gene family in wheat (*Triticum aestivum* L.) and characterization of TaCPK40 associated with seed dormancy and germination. Plant Physiol Biochem. 2023;196:608–623. https://doi.org/10.1016/j.plaphy.2023.02.014.
48. Zhang YY, Huang XY, Zhang L, Gao WD, Ma JF, Chen T, Yang DL. Genome-wide identification, gene expression and haplotype analysis of the gene family in wheat (*Triticum aestivum* L.). Plant Genome. 2024. https://doi.org/10.1002/tpg2.20435.
49. Wu Y, Wen J, Xia YP, Zhang LS, Du H. Evolution and functional diversification of R2R3-MYB transcription factors in plants. Horticulture Res. 2022;9. https://doi.org/10.1093/hr/uhac058.
50. Qiao X, Li QH, Yin H, Qi KJ, Li LT, Wang RZ, Zhang SL, Paterson AH. Gene duplication and evolution in recurring polyploidization-diploidization cycles in plants. Genome Biology. 2019;20(1). https://doi.org/10.1186/s13059-019-1650-2.
51. Cuevas HE, Zhou CB, Tang HB, et al. The Evolution of Photoperiod-Insensitive Flowering in Sorghum, A Genomic Model for Panicoid Grasses. Mol Biol Evol. 2016;33(9):2417–28. https://doi.org/10.1093/molbev/msw120.
52. Wang XY, Gowik U, Tang HB, Bowers JE, Westhoff P, Paterson AH. Comparative genomic analysis of C4 photosynthetic pathway evolution in grasses. Genome Biol. 2009;10(6). https://doi.org/10.1186/gb-2009-10-6-r68.
53. Blanc G, Wolfe KH. Functional Divergence of Duplicated Genes Formed by Polyploidy during *Arabidopsis* Evolution [W]. Plant Cell. 2004;16(7):1679–91. https://doi.org/10.1105/tpc.021410.
54. Maere S, De Bodt S, Raes J, Casneuf T, Van Montagu M, Kuiper M, Van de Peer Y. Modeling gene and genome duplications in eukaryotes. Proc Natl Acad Sci USA. 2005;102(15):5454–9. https://doi.org/10.1073/pnas.0501102102.
55. Zhang YM, Liu ZS, Khan A, et al. Expression partitioning of homeologs and tandem duplications contribute to salt tolerance in wheat (*Triticum aestivum* L.). Sci Rep. 2016;6(1). https://doi.org/10.1038/srep21476.
56. Dossa K, Diouf D, Cissé N. Genome-Wide Investigation of Hsf Genes in Sesame Reveals Their Segmental Duplication Expansion and Their Active Role in Drought Stress Response. Front Plant Sci. 2016;7. https://doi.org/10.3389/fpls.2016.01522.
57. Morcuende R, Bari R, Gibon Y, et al. Genome-wide reprogramming of metabolism and regulatory networks of *Arabidopsis* in response to phosphorus. Plant, Cell Environ. 2006;30(1):85–112. https://doi.org/10.1111/j.1365-3040.2006.01608.x.
58. Zhang Z, Liao H, Lucas WJ. Molecular mechanisms underlying phosphate sensing, signaling, and adaptation in plants. J Integr Plant Biol. 2014;56(3):192–220. https://doi.org/10.1111/jipb.12163.
59. Lu H, Wang F, Wang Y, Lin RB, Wang ZY, Mao CZ. Molecular mechanisms and genetic improvement of low-phosphorus tolerance in rice. Plant Cell Environ. 2023;46(4):1104–19. https://doi.org/10.1371/journal.pgen.1009197.
60. Yan L, Su L, Li R, Li H, Bai JR, Sun FJ. Differential Gene Expression Responding to Low Phosphate Stress in Leaves and Roots of Maize by cDNA-SRAP. Biomed Res Int. 2020;2020:1–13. https://doi.org/10.1155/2020/8420151.
61. Puga MI, Mateos I, Charukesi R, et al. SPX1 is a phosphate-dependent inhibitor of phosphate starvation response 1 in *Arabidopsis*. Proc Natl Acad Sci USA. 2014;111(41):14947–52. https://doi.org/10.1073/pnas.1404654111.
62. Lim PK, Zheng XH, Goh JC, Mutwil M. Exploiting plant transcriptomic databases Resources, tools, and approaches. Plant Commun. 2022;3(4). https://doi.org/10.1016/j.xplc.2022.100323.
63. Chang MX, Gu M, Xia YW, et al. OsPHT1;3 Mediates Uptake, Translocation, and Remobilization of Phosphate under Extremely Low Phosphate Regimes. Plant Physiol. 2019;179(2):656–70. https://doi.org/10.1104/pp.18.01097.
64. Nguyen NNT, Clua J, Vetal PV, Vuarambon DJ, De Bellis D, Pervent M, Lepetit M, Udvardi M, Valentine AJ, Poirier Y. PHO1 family members transport phosphate from infected nodule cells to bacteroids in *Medicago truncatula*. Plant Physiol. 2021;185(1):196–209. https://doi.org/10.1093/plphys/kiaa016.
65. Mani B, Maurya K, Kohli PS, Giri J. Chickpea (*Cicer arietinum*) PHO1 family members function redundantly in Pi transport and root nodulation. Plant Physiol Biochem. 2024;211: 108712. https://doi.org/10.1016/j.plaphy.2024.108712.
66. Secco D, Baumann A, Poirier Y. Characterization of the rice PHO1 gene family reveals a key role for OsPHO1;2 in phosphate homeostasis and the evolution of a distinct clade in dicotyledons. Plant Physiol. 2010;152(3):1693–704. https://doi.org/10.1104/pp.109.149872.
67. He K, Du J, Han X, Li H, Kui M, Zhang J, Huang Z, Fu Q, Jiang Y, Hu Y. Phosphate starvation response1 (PHR1) interacts with Jasmonate Zim-Domain (JAZ) and MYC2 to modulate phosphate deficiency-induced jasmonate signaling in *Arabidopsis*. Plant Cell. 2023;35(6):2132–2156. https://doi.org/10.1093/plcell/koad057.
68. Ren F, Guo QQ, Chang LL, Chen L, Zhao CZ, Zhong H, Li XB. *Brassica napus* PHR1 gene encoding a MYB-like protein functions in response to phosphate starvation. PLoS ONE. 2012;7(8):e44005. https://doi.org/10.1371/journal.pone.0044005.
69. Duan K, Yi KK, Dang L, Huang HJ, Wu W, Wu P. Characterization of a sub-family of *Arabidopsis* genes with the SPX domain reveals their diverse functions in plant tolerance to phosphorus starvation. Plant J. 2008;54(6):965–75. https://doi.org/10.1111/j.1365-313X.2008.03460.x.
70. Qu L-J, Ueda Y, Nosaki S, Sakuraba Y, Miyakawa T, Kiba T, Tanokura M, Yanagisawa S. NIGT1 family proteins exhibit dual mode DNA recognition to regulate nutrient response-associated genes in *Arabidopsis*. PLOS Genet. 2020;16(11). https://doi.org/10.1371/journal.pgen.1009197.
71. Ueda Y, Kiba T, Yanagisawa S. Nitrate-inducible NIGT1 proteins modulate phosphate uptake and starvation signaling via transcriptional regulation of SPX genes. Plant J. 2020;102(3):448–66. https://doi.org/10.1111/tpj.14637.

Publisher's Note